Correlations among global photometric properties of disk galaxies

Habib G. Khosroshahi [1]
Institute for Advanced Studies in Basic Sciences, P. O. Box 45195-159 Zanjan, Iran
Yogesh Wadadekar [2] and Ajit Kembhavi [3]
Inter University Centre for Astronomy and Astrophysics, Post Bag 4, Ganeshkhind, Pune 411007, India

ABSTRACT

Using a two-dimensional galaxy image decomposition technique, we extract global bulge and disk parameters for a complete sample of early type disk galaxies in the near infrared K band. We find significant correlation of the bulge parameter n with the central bulge surface brightness $\mu_b(0)$ and with effective radius r_e. Using bivariate analysis techniques, we find that $\log n$, $\log r_e$ and $\mu_b(0)$ are distributed in a plane with small scatter. We do not find a strong correlation of n with bulge-to-disk luminosity ratio, contrary to earlier reports. r_e and the disk scale length r_d are well correlated for these early type disk galaxies, but with large scatter. We examine the implications of our results to various bulge formation scenarios in disk galaxies.

Subject headings: galaxies: fundamental parameters — galaxies: spiral — galaxies: structure — infrared: galaxies

[1]khosro@iasbs.ac.ir
[2]yogesh@iucaa.ernet.in
[3]akk@iucaa.ernet.in

1. Introduction

Accurate photometric and kinematic modeling of galactic morphology is a prerequisite for tackling the many unresolved problems regarding the formation and evolution of galaxies, e.g. the formation of bulges in disk galaxies. There are two popular scenarios for the formation of such bulges: In the first scenario, the bulge and the disk are formed independently, in the second the disk forms first and the bulge forms later by secular evolution. A quantitative evaluation of the plausibility of such formation scenarios requires accurate extraction of global parameters that describe the luminosity and density distribution of the bulge as well as the disk.

Following the path breaking work of de Vaucouleurs (1948), the empirical law named after him was extensively used to describe the light distribution in elliptical galaxies and in the bulges of spiral galaxies (de Vaucouleurs 1959). With the advent of more accurate CCD surface photometric techniques, systematic deviations from the $r^{1/4}$ law for ellipticals were extensively reported in the literature (Michard 1985, Schombert 1986, van den Bergh 1989, Bingelli & Cameron 1991). Alternative descriptions that emerged included the $r^{1/n}$ law, with n as a free parameter, first proposed by Sersic (1968). This generalized de Vaucouleurs law was used to fit a sample of elliptical and S0 galaxies by Caon, Cappacioli & D'Onofrio (1993) who found a large range of values in n, with n correlated with the effective radius and the total luminosity of the galaxy. More recently, Andredakis, Peletier & Balcells (1995, hereafter APB95) used the $r^{1/n}$ law to fit the bulges of spiral galaxies. They found that n varies systematically from values around 1 (which corresponds to an exponential) to 6, from late to early type bulges; the profiles fall off less steeply near the center (i.e. have lower n values), in the later types. de Jong (1996) also reported that the bulges of late type galaxies are better fit by an exponential than the de Vaucouleurs' law.

The standard description for the light profile of the disk component is an exponential, first proposed by Freeman (1970). It has been found that an exponential profile also describes the light distribution in the disks of S0s (Burstein 1979). An inner truncated exponential disk has been proposed (Kormendy 1977a) to describe the disk profile, but is not widely used.

After the photometric parameters describing the bulge and disk have been extracted, the next step is to look for correlations between them. Such correlations have been investigated by several authors (e.g. Kormendy 1977a; Schombert & Bothun 1987; APB95; Courteau, de Jong & Broeils 1996; de Jong 1996; Bingelli & Jerjen 1998). In this paper, we examine correlations among the bulge and disk parameters for a complete magnitude limited sample of high inclination disk galaxies using the $r^{1/n}$ law to model the bulge and an exponential law to model the disk.

This paper is organized as follows: in Section 2 we describe the data set and the decomposition procedure used to obtain the bulge and disk parameters. Section 3 contains a detailed description of the fitting and a comparison with values reported in the literature. Various correlations observed between bulge and disk parameters are discussed in Section 4. Section 5 contains the conclusions.

2. The data

2.1. Sample definition

The galaxies that we use are from a complete, diameter-limited, optically selected sample of early to intermediate type spirals from the UGC catalogue. The sample was constructed by Balcells and Peletier (1994), where details about selection criteria may be found. The sample is complete for the specified galaxy types and diameter and magnitude ranges. Thirty objects from this sample were studied by APB95; the details of the observations are given in Peletier and Balcells (1997) and APB95. We have used their reduced K band images publicly available at the New Astronomy journal website[4], in this work. The data at the website are identical to that described in APB95 except that they have been rebinned to a pixel scale of 0.549 arcsecond, which was the scale used for observations in the $UBRI$ bands. The data reduction procedures are described in detail in Peletier & Balcells (1997) and APB95.

The main morphological criteria for the sample selection were that the major axis diameter should be > 2 arcmin, and the axial ratio in the B filter should be > 1.56, which corresponds to disk inclinations > 50 degrees. Such a constraint on axial ratio was necessary to the specific bulge disk decomposition technique employed in APB95, which requires that the apparent ellipticities of the bulge and the disk be as distinct as possible. The sample is thus biased in ori-

[4] http://www.elsevier.nl/

entation, towards edge-on galaxies. Of the 30 galaxies we have used only 26, for reasons cited in Section 3. The morphological type index of these galaxies was obtained from the RC3 catalog (de Vaucouleurs et al. 1991) while the apparent magnitude m and redshift z were obtained from the NASA Extragalactic Database (NED). These quantities are listed in Table 1.

2.2. The decomposition procedure

Extracting the structural parameters of a galaxy requires the separation of the observed light distribution into bulge and disk components. There is considerable variation in the details of the decomposition techniques proposed by various researchers. In recent years, novel methods that employ two dimensional fits to broad band galaxy images have been proposed (eg. Byun & Freeman 1995; de Jong 1996; Wadadekar, Robbason and Kembhavi 1999) as alternatives to conventional one dimensional techniques, where the bulge and the disk models are fit either iteratively or simultaneously to a one dimensional surface brightness profile (e.g. Kormendy 1977a; Kent 1985; Simien & de Vaucouleurs 1986; Schombert & Bothun 1987; Baggett, Baggett & Anderson 1998). Most of these decomposition techniques assume specific surface brightness distributions like the de Vaucouleurs' law for the bulge and an exponential distribution for the disk. A notable exception is the method proposed by Kent (1985), which can perform the decomposition in a model independent way. However, extraction of global parameters that quantitatively describe the bulge and the disk, still requires use of a model. APB95 use a two dimensional generalization of Kent's method to extract their parameters.

Our decomposition procedure is a full two dimensional method that uses information from all pixels in the image. It essentially involves a numerical solution to a signal-to-noise weighted χ^2 minimization problem. We achieve this minimization using the Davidon-Fletcher-Powell variable metric algorithm included as part of MINUIT – a multidimensional minimization package from CERN (James 1994). Our technique involves building two dimensional image models that best fit the observed galaxy images with the quality of the fit evaluated by the χ^2 value. The weights for the χ^2 function are computed using the S/N ratio at each pixel of the galaxy image. The model image is convolved with the measured PSF from the galaxy frame before the χ^2 is computed. Details of the accuracy and reliability of the decomposition procedure, and the associated galaxy simulation code, are provided in Wadadekar et al. (1999) and will not repeated here.

Working with K band data for decomposition is easier and more effective than the visible bands, because of a relative lack of absorption related features in the near infrared. The smooth, featureless light profiles of galaxies in this band are very convenient for extraction of global disk and bulge parameters. Use of K band data is especially important for our sample, as it includes several dusty galaxies. In our bulge-disk decomposition, we have the following as free parameters: (1) $I_b(0)$: the central bulge intensity, in counts, which can later be converted to mag arcsec^{-2} (2) r_e: the half light radius of the bulge in pixels (3) e_b: the ellipticity of the bulge (4) n: the bulge shape parameter (5) $I_d(0)$: the central intensity of the disk in counts (6) r_d: the scale length of the disk in pixels (7) e_d: the ellipticity of the disk

With these definitions the bulge intensity distribution can be written as

$$\begin{aligned} I_{bulge}(x,y) &= I_b(0)e^{-2.303b_n(r_{bulge}/r_e)^{1/n}}, \quad (1) \\ r_{bulge} &= \sqrt{x^2 + y^2/(1-e_b)^2}, \end{aligned}$$

where x and y are the distances from the center of the galaxy along the major and minor axis respectively and b_n is a function of n which is a root of an equation involving the incomplete gamma function. However, a simplification can be introduced in the procedure because b_n can be expressed as a linear function of n, accurate to better than one part in 10^5, by

$$b_n = 0.868242\,n - 0.142058.$$

For $n = 4$, which corresponds to de Vaucouleurs law, $b_4 = 3.33$.

The projected disk profile is represented by an exponential distribution,

$$\begin{aligned} I_{disk}(x,y) &= I_d(0)e^{-r_{disk}/r_d}, \quad (2) \\ r_{disk} &= \sqrt{x^2 + y^2/(1-e_d)^2}. \end{aligned}$$

The ellipticity of the disk in the image is due to projection effects alone and is given by

$$e_d = 1 - \cos(i), \quad (3)$$

where i is the angle of inclination between the line of sight and the normal to the disk plane.

The bulge-to-disk luminosity ratio is a parameter which is commonly used as a quantitative measure for morphological classification of galaxies. For the $1/n$ law it is given by

$$(B/D)_n = \frac{n\Gamma(2n)}{(2.303b_n)^{2n}} \left(\frac{I_b(0)}{I_d(0)}\right) \left(\frac{r_e}{r_d}\right)^2. \quad (4)$$

For $n = 4$ this reduces to the familiar result from Mihalas and Binney (1981),

$$(B/D)_4 = \frac{1}{0.28} \left(\frac{I_b(r_e)}{I_d(0)}\right) \left(\frac{r_e}{r_d}\right)^2, \quad (5)$$

Note that we use $I_b(r_e)/I_d(0)$ in the above equation, where $I_b(r_e) = 10^{-3.33} I_b(0)$ is the intensity at the half–light radius, in place of $I_b(0)/I_d(0)$ used in Equation 4.

3. Decomposition results

We were able to obtain satisfactory fits with a reduced $\chi^2_\nu < 2$ for 26 of the 30 galaxies in the APB95 sample. We were unable to get a good decomposition for 4 galaxies: NGC 5389, NGC 5443, NGC 5577 and NGC 5746. This is very likely because of the fact that all these galaxies show significant departure from twofold symmetry, in the high S/N regions near the center of the galaxy. The constant (ie, unchanging with radius) and equal position angle that we assume for the bulge and disk components, which implies a twofold symmetry, is not a valid assumption for these objects. Since our decomposition does not give us a fit with a satisfactory reduced χ^2_ν for these galaxies we have not used them in our analysis. Our subsequent discussion only applies to the remaining 26 galaxies, for which we have been able to obtain a satisfactory fit. Our extracted parameter values for these 26 galaxies are presented in Table 1. Error on the bulge parameter n represented by Δn is also listed. This error was computed by MINUIT from the Hessian error matrix, which is the inverse of the matrix of second derivatives of the χ^2 function, with respect to the variable parameters.

Accurate estimation of the full width at half maximum (FWHM) of the point spread function (PSF) is crucial to our decomposition procedure because we give maximum weightage to the high S/N points near the centre of the galaxy. This is especially true if the scale length in angular terms is comparable to the seeing FWHM. The central galaxy pixels are affected the most by convolution with the (possibly inaccurate) PSF. The FWHM is usually computed using the brightest unsaturated stars in the image. In our data set only 12 galaxy images contain suitable bright stars in the field and their FWHM ranges from 0.9 to 1.2 arcsec. For the other 14 objects, it is not possible to directly measure the FWHM. In order to estimate the FWHM for these galaxies, we took test runs with the value of the FWHM set to 0.8, 1.0 and 1.2 arcsecond and tried to fit all 14 galaxies with these values to see how various parameters, especially those of the bulge, are affected by an erroneous estimation of the PSF. Changing the FWHM within this range does not change the results significantly. In the extreme case, changing from 0.8 to 1.2 arcsecond, the extracted parameters do not show a discrepancy larger than about 10 percent. This fortunate circumstance in our sample is due to the fact that bulge effective radii are $\geq 3\times$ FWHM for all except four galaxies which have bulge effective radii of about 1.75 FWHM. We used an FWHM of 1.0 arcsecond in our analysis of all 26 galaxies.

3.1. Comparison with APB95 results

We have compared parameter values from APB95 with those obtained in this work for the same sample. We use $H_0 = 50\,\mathrm{km\,sec^{-1}\,Mpc^{-1}}$ and $q_0 = 0.5$, throughout this paper. Figure 1 shows plots of values extracted by us compared to the values reported in APB95 for each parameter. The diagonal line in each plot represents a perfect match between the two sets of values.

Ellipticity of the bulge and disk are rather stable parameters in the fitting process. These parameters are never affected by the choice of initial values and can usually be extracted with a small error. APB95 claim that it is not easy to extract bulge ellipticities by any method, and errors of the order of 30 percent are possible. As we have already pointed out in Wadadekar et al. (1999), our decomposition method allows us to extract bulge ellipticities with much better accuracies (to better that 5 percent accuracy in 95 percent of simulated test galaxies). We wish to emphasize here that our technique is different from that used in APB95 and it does not require the precondition that apparent ellipticities of bulge and disk be as distinct as possible.

Comparison of extracted values of the shape parameter n of the bulge shows that for 14 galaxies out of 26, our error bar for n overlaps with the error bar

on the corresponding n values reported in APB95. The deviation for most of the remaining galaxies is not large.

The bulge effective radius is consistently estimated overall. However, for the larger bulges, our value is systematically higher than the APB95 value by about 20 percent.

The authors of APB95 have not reported the values of the disk scale length in their paper. However, in a subsequent paper presenting their data (Peletier & Balcells 1997), they employed a different technique to measure the disk scale length. They extracted the disk scale length from the disk profile computed by azimuthally averaging the total light of the galaxy (including light from both the bulge and the disk components), in a wedge with full width of 10 degrees, placed slightly away from each semi-major axis. Such a technique leads to contamination from the bulge light in the central parts. This "extra" light at the center leads to a consistent underestimation of disk scale length by their technique, as shown in panel (d) of Figure 1.

4. Correlations

The next step in testing of predictions made by theoretical models for the formation and evolution of galaxies, is to look for correlations between global photometric parameters. Several such correlations have been reported in the literature. These correlations are useful in reducing the number of free parameters that characterize galaxies, making the analysis easier. One such correlation was found by Kormendy (1977b) for large ellipticals by fitting the galaxy profiles with the $r^{1/4}$ law. It relates the central surface brightness B_0 in the B band measured in mag arcsec^{-2} to the half light radius r_e,

$$B_0 = 3.02 \log r_e + 19.74\,. \qquad (6)$$

The constants in this equation were determined by Kormendy using a least square fit to the galaxy profiles. Subsequent work (eg. Djorgovski & Davis 1987) found that the mean surface brightness within the effective radius, $\langle SB \rangle_{eff}$, was a better parameter to use than the central surface brightness in the Kormendy relation, as it is affected less by measurement errors. Such a relation is free of model dependent parameters because both $\langle SB \rangle_{eff}$ and r_e can be measured operationally, without assuming a specific form for the luminosity profile of the galaxy.

For a de Vaucouleurs elliptical, it can be shown that

$$L \propto I_b(0) {r_e}^2 \propto I_b(r_e) {r_e}^2, \qquad (7)$$

where L is the luminosity and $I_b(r_e) = 10^{-3.33}\, I_b(0)$. For galaxies obeying Equation 6 and Equation 7, the luminosity of elliptical galaxies reduces to a one parameter family. For the $1/n$ law the luminosity is given by

$$L \propto I_b(r_e) {r_e}^2\, \psi(n), \qquad (8)$$

where

$$\psi(n) = \frac{n\Gamma(2n) e^{2.303 b_n}}{(2.303 b_n)^{2n}}. \qquad (9)$$

Using the Kormendy relation, the luminosity of elliptical galaxies now reduces to a two parameter family.

In recent years, there have been attempts to correlate the n parameter of bulges with other observables, with mixed success. Caon et al. 1993 reported a correlation of n with luminosity as well as effective radius, while APB95 reported a correlation between n and morphological type and between n and the B/D luminosity ratio. The parameter n measures the steepness of the luminosity profile of the bulge. This is illustrated in Figure 2, where we present surface brightness profiles in arbitrary units for a $r^{1/n}$ galaxy with $I_b(0) = 1$ for $n = 1, 4, 7$. It is seen that as n increases, the steepness of the profile increases rapidly near the centre, while for $r > r_e$ the profiles become flatter with increasing n. If the value of n is very large, say $n = 16$, the largest value reported by Caon et al. (1993) for giant ellipticals, the profile is so steep that a very large value of $I_b(0)$ would be required to prevent the galaxy from disappearing into the background within a very short distance from its centre. From Equation 8 it follows that a galaxy with high n would have a high luminosity such as is found only among giant ellipticals. Such a trend has been observed in a sample of 119 Abell brightest cluster galaxies by Graham et al. (1996).

We shall first consider correlations among bulge and disk parameters separately and then correlations involving both bulge and disk parameters.

4.1. Correlations among bulge parameters

4.1.1. Univariate correlations

Here we consider the three bulge parameters n, $\mu_b(0)$ and r_e, taken two at a time. We find that there is good correlation between effective radius and

n as shown in Figure 3. The linear correlation coefficient is 0.61 with a significance level of 99.98 percent. There is an even stronger correlation between n and the bulge central surface brightness as shown in Figure 4. The linear correlation coefficient in this case is -0.88 at a significance level better than 99.99 percent. There is no significant correlation between $\mu_b(0)$ and r_e. The Kormendy relation between $\langle SB \rangle_{eff}$ and r_e would imply a correlation between $\mu_b(0)$ and r_e, if a simple offset exists between $\mu_b(0)$ and $\mu_b(r_e)$ as in ellipticals following the de Vaucouleurs law. When the parameter n is introduced, the relation between $\mu_b(0)$ and $\mu_b(r_e)$ is strongly dependent on n because $\mu_b(0) = \mu_b(r_e) - 2.5\, b_n$ and therefore there is no correlation between $\mu_b(0)$ and r_e, in spite of the Kormendy relation.

4.1.2. Bivariate correlations and a new fundamental plane?

Since univariate correlations exist but with large scatter, there is the possibility that some of the scatter may be caused by the effects of a third parameter.

The methods of multivariate statistics can be applied here to the three bulge parameters n, $\mu_b(0)$ and r_e. We obtain a least square fit of two of these quantities and correlate residuals from the fit with the third quantity. If the residuals show significant correlation with the third quantity, we make a linear combination of that quantity and one of the previous two, and optimize the fit again. We have used the MINUIT minimization program (James 1994) for this optimization. The quality of the fit is judged by the χ^2 value and the value of the linear regression coefficient. After such bivariate analysis using all possible combinations for the three variables, we find that the best fit is obtained by expressing $\log n$ as a linear combination of the other two parameters. The best fit plane is:

$$\begin{aligned} \log n &= (0.130 \pm 0.040) \log r_e - (0.073 \pm 0.011)\mu_b(0) \\ &+ (1.21 \pm 0.11) \end{aligned} \quad (10)$$

which corresponds to a scaling law:

$$n \sim I_b(0)^{0.183 \pm 0.028}\, r_e^{0.130 \pm 0.040} \quad (11)$$

The fit is shown in Figure 5. The scatter in the plot is small, 0.058 dex in $\log n$. This is equivalent to a scatter of $2.5 \times 0.058 = 0.145$ in magnitude units.

We explored to what extent these correlations are caused by a coupling of the errors associated with the model parameters due to the parameters compensating each other, as each parameter changes. If such is the case, the bivariate correlation would not be as significant as it appears. We used a Monte-Carlo like simulation technique, where we simulated galaxy images with the same parameter distributions as that of the sample galaxies. We tested to see to what extent a correlation appears in the fitted parameters, when there is no correlation in the input parameters to the simulation program. We found that no artificial univariate or bivariate correlations are generated (Khosroshahi, Wadadekar & Kembhavi, under preparation).

Such a tight correlation involving these three purely photometric parameters has not been noticed previously and is the main result of this paper.

4.2. Univariate Correlations among disk parameters

The light distribution in the disk is defined by just two parameters, the disk central surface brightness, $\mu_d(0)$ and r_d. An anti-correlation is seen between these two quantities as shown in Figure 6 but the scatter is large. The linear correlation coefficient between $\mu_d(0)$ and $\log r_d$ is 0.645 with a significance of 99.96 percent.

4.3. Bulge-disk correlations

4.3.1. $\log n - \log(B/D)$ correlation

A strong correlation of $\log n$ with $\log(B/D)$ with a correlation coefficient of 0.54 and significance of 99.7 percent for 30 galaxies has been reported in APB95. In our work, we find that the $\log n - \log(B/D)$ correlation is weak with a linear correlation coefficient of 0.30 and a significance level of only 86.5 percent (See Figure 7). Note that these results are obtained when we consider the 26 galaxies for which we have a good fit. Using APB95 results for the same 26 galaxies, we get a correlation coefficient of 0.55 with a significance level of 99.7 percent. We believe that the marked difference between our results and those of APB95 may be due to the fact that APB95 used a different technique to estimate the disk contribution. The disk magnitude used in their B/D luminosity ratio was determined by straightforward integration of the disk profile until the last measured point. The disk profile was obtained by simply subtracting the bulge profile from the total major axis profile. In such a technique any errors in determination of the bulge profile would

get transferred to the disk profile directly.

A better correlation is seen between $\log n$ and bulge luminosity. We show such a plot in Figure 8, where the absolute K magnitude of the bulge is used as a measure of its luminosity. This correlation is tighter than our $\log n - \log(B/D)$ correlation with linear correlation coefficient -0.40 with a significance of 95.9 percent. However the scatter is quite large.

We have shown in Figure 9 a plot of $\log n$ against the morphological type taken from the RC3 (de Vaucouleurs et al. 1991) catalog. Since our sample consists of edge-on galaxies, it is difficult to determine their morphological type using criteria involving spiral arms. In spite of this problem a trend is seen with the later morphological types having smaller values of n. But the formal correlation coefficient between $\log n$ and morphological type index T is low, essentially because of the cluster of points with high n and $T = 3$. APB95 found a tighter correlation between the two parameters (see their Figure 5(a)), but much of the correlation there is due to the data points from Kent (1986), where the morphological classification is more reliable because the galaxies are less edge-on.

4.3.2. $r_e - r_d$ correlation

An interesting correlation between bulge and disk scale lengths was reported by Courteau, de Jong and Broeils (1996). They used two samples of late type spiral galaxies, one from Broeils and Courteau (1996) and the other from de Jong (1996). They modeled the bulge keeping the shape parameter fixed at $n = 1$ and obtained the bulge scale length r_b for their exponential fit. For $n = 1$, r_b is related to the effective radius r_e by $r_e = 1.679\, r_b$. For 83 galaxies from the de Jong sample they found a mean r_b/r_d ratio in the R band of 0.072 ± 0.043 (equivalent to a mean r_e/r_d ratio of 0.121 ± 0.072) whereas for 243 galaxies from the Broeils and Courteau sample they found a mean r_b/r_d ratio of 0.082 ± 0.053 (equivalent to a mean r_e/r_d ratio of 0.138 ± 0.089), also in the R band. Such a relationship between bulge and disk scale lengths is best understood in models where the disk forms first and the bulge emerges later from the disk. In such models, the exponential disk is formed by the redistribution of angular momentum by viscous evolution, provided that star formation occurs on roughly the same timescale. A bulge emerges naturally in such a scheme and its properties depend only on the relative timescales of star formation and viscous transport and on the total angular momentum (Combes et al. 1990; Saio & Yoshi 1990; Struck-Marcell 1991). Correlated bulge and disk scale lengths are predicted by these models (Courteau et al. 1996).

A comparison between our distribution of r_e/r_d in the K band with earlier results can be made using results from de Jong (1996). He obtained a mean value of $(r_e/r_d)_K$ of 0.15 ± 0.05, again for $n = 1$ fixed, for his sample of predominantly late type face-on disk galaxies. The corresponding value for our sample of predominantly early type edge-on disk galaxies is 0.33 ± 0.17. A Student's t-test reveals that the means for the two samples are different a significance level of 99.5 percent. This indicates that the ratio r_e/r_d is not constant over the entire population of disk galaxies. A recent statistical analysis of the the de Jong sample by Graham & Prieto (1999) has demonstrated that the scale length ratio does indeed vary with Hubble type. These results lend observational support to the hypothesis that more than one bulge formation mechanism may be at work. As suggested by Courteau et al. (1996) it may be possible that early type and late type disk galaxies were formed by different physical mechanisms - big bulges (> 2 kpc as in Sa galaxies) formed principally from a minor merger and smaller bulges formed mainly via secular evolution.

In Figure 10, we plot the bulge effective radius against the disk scale length, with points from our sample shown as filled circles and those from the K band observations of de Jong (1996) as open circles. From the plot it is apparent that the disk scale lengths of our sample and the de Jong sample span the same range, but our bulge effective radii are larger on the average (which is to be expected in early type galaxies) giving us a mean r_e/r_d ratio that is about 2.2 times larger than the de Jong value.

We next test the dependence of the scale length ratio on morphological type. In Figure 11 we show a plot of the two parameters. There is no indication in the plot of a dependence of the scale length on morphological type and the formal correlation coefficient is not significant. However, the scatter is large. Some of this scatter could be due to incorrect morphological type classification, due to the edge-on nature of the galaxies. The plot should be reexamined with a sample of galaxies with more secure morphological classification.

4.3.3. Other Correlations

A plot of $\log B/D$ against morphological type in Figure 12 shows an anti-correlation which is significant at the 97.8 percent level. This is not surprising as the variation of the B/D luminosity ratio with morphological type is supposed to be an important characteristic of the the Hubble sequence, with the ratio decreasing towards the later Hubble types.

We have shown in Figure 13 a plot of $\log(I_b(0)/I_d(0))$ against morphological type for our sample. A clear dependence is seen which is particularly striking if we ignore the points at $T = 3$. The linear correlation coefficient for all 26 points is -0.36, which is significant at the 92.8 percent level. Omitting the eight points at $T = 3$, the correlation coefficient improves to -0.75 and the significance to 99.97 percent. The decrease in the B/D luminosity ratio towards the later morphological types is driven by this decrease in $I_b(0)/I_d(0)$. because r_e/r_d does not depend strongly on morphological type as is seen in Figure 11.

If the bulges of early and late type disk galaxies did indeed form by different mechanisms, then there should exist other observable differences in the bulge properties of early and late type disk galaxies. We test this idea by plotting the surface brightness at the effective radius r_e as a function of bulge effective radius for our sample which is dominated by *early* type disk galaxies and that of de Jong (1996) which contains mostly *late* type disk galaxies. Figure 14 shows our points as filled circles and the points from de Jong (1996) as open circles. This plot can be viewed in conjunction with Fig. 7(b) in APB95 to see a trend: bulges of early type disk galaxies seem to obey a linear Kormendy type relation, albeit with large scatter, suggesting a formation scenario similar to that of ellipticals. On the other hand, bulges of late type spirals are widely scattered mostly below this line, suggesting a different formation history, with secular evolution being one of the possibilities. We will explore this trend further in a future paper using K band data on a sample of elliptical galaxies.

The authors of APB95 rejected secular evolution models on the basis of their continuous spectrum of the index n versus morphological type and B/D luminosity ratio. They proposed that the smooth sequence they observed, in their Fig. 5, is an indicator of a single mechanism of bulge formation in all disk galaxies. We have found that neither B/D luminosity ratio nor morphological type correlate with n as strongly as APB95. Additionally, as pointed out by Courteau et al. (1996), the scatter in the plot is too large to justify the APB95 claim. In such a situation, ruling out the possibility of secular evolution is not warranted. The present data are too sparse to test for any bimodality in the variation of n with morphological type.

Observationally these scenarios can be differentiated by studying the evolution of B/D luminosity ratio and colors of galaxies with redshift. A series of schematic models have been developed using the data from APB95 and de Jong (1996) by Bouwens, Cayon & Silk (1999). Unfortunately, currently available high z galaxy observations have small sample sizes and the measurement uncertainties are too large to test the predictions of these models.

5. Conclusions

The bulge shape parameter n is separately correlated with both the bulge effective radius and the bulge central surface brightness. A larger value of n implies a larger bulge which is also brighter at the centre. A strong correlation between n and the bulge-to-disk luminosity ratio was reported in APB95. We do not find a correlation as strong as theirs in our work. A strong bivariate correlation between bulge central surface brightness, bulge effective radius and n exists with a scatter as small as 0.058 dex in $\log n$. Such a tight best fit plane is the first bivariate correlation noted involving these three purely photometric parameters. The physical implications of this correlation need to be explored by analytic and numerical techniques.

The bulge and disk scale lengths are correlated, but the scatter is large indicating that more than one bulge formation mechanism may be at work with a possible dependence on morphological type. In contrast to the findings of Courteau et al. (1996) and in agreement with the conclusions of Graham & Prieto (1999), the mean scale length ratio does seem to change with morphological type. The disk central surface brightness and disk scale length are anti-correlated.

A detailed near infrared study of a complete sample of elliptical galaxies is underway, as a complementary study to the present work. The results from that study will enable us to compare and contrast the photometric properties of the bulges of spirals and ellipticals, and study in detail what effect the presence of

a disk has on the global parameters of the bulges of disk galaxies. It would be interesting to see if a bivariate relation, of the form described in this work, also holds for elliptical galaxies.

We thank Y. C. Andredakis, R.F. Peletier and M. Balcells for making their data publicly available. We thank S. George Djorgovski and the referee, Alister Graham for several helpful comments and suggestions.

This research has made use of the NASA/IPAC Extragalactic Database (NED) which is operated by the Jet Propulsion Laboratory, California Institute of Technology, under contract with the National Aeronautics and Space Administration.

REFERENCES

Andredakis, Y.C., Peletier, R.F., & Balcells, M. 1995, MNRAS, 275, 874
Balcells, M. & Peletier, R.F. 1994, AJ, 107, 135
Baggett, W.E., Baggett, S.M., & Anderson, K.S.J. 1998, AJ, 116, 1626
Bingelli, B., & Cameron, L.M. 1991, A&A, 252, 27
Bingelli, B., & Jerjen, H. 1998, A&A, 333, 17
Bouwens, R., Cayon, L. & Silk, J. 1999, ApJ, 516, 77
Burstein, D. 1979, ApJS, 41, 435
Byun, Y.I., & Freeman, K. 1995, ApJ, 448, 563
Caon, N., Capaccioli, M. & D'Onofrio, M. 1993, MNRAS, 163,1013
Combes, F., Debbash, F., Friedli, D., & Pfenniger, D. 1990, A&A, 233, 82
Courteau, S., de Jong, R. S. & Broeils, A. H. 1996, ApJ, 457, L73
de Jong R. S. 1996, A&AS, 118, 557
de Vaucouleurs, G. 1948, Ann. d'Astrophys., 11, 247
de Vaucouleurs, G. 1959, Hdb. d. Physik, 53, 311
de Vaucouleurs, G. *et al*, 1991, Third Reference Catalog of Bright Galaxies (New York: Springer) (RC3)
Djorgovski, S.G. & Davis, M. 1987, ApJ, 313 , 59
Freeman, K. 1970, ApJ, 160, 811
James, F. 1994, MINUIT: Function Minimization and Error Analysis (CERN Program Libr. Long Writeup D506) (version 94.1; Geneva: CERN)
Graham, A. W., & Prieto, M. 1999, ApJ, 524, L23
Graham, A., Lauer, T. R., Colless, M. & Postman, M. 1996, ApJ, 465, 534
Kent, S.M. 1985, ApJS, 59, 115
Kent, S.M. 1986, AJ, 91, 1301
Kormendy, J. 1977a, ApJ, 217, 406
Kormendy, J. 1977b, ApJ, 218, 333
Michard, R. 1985, A&A, 59, 205
Mihalas D. & Binney J. 1981, Galactic Astronomy (New York: W. H. Freeman and Company)
Peletier, R.F., & Balcells, M. 1997, New Astronomy, 1, 349
Saio, H., & Yoshii, Y. 1990, ApJ, 363, 40
Schombert, J. M. 1986, ApJ, 60, 603
Schombert, J., & Bothun, G. D. 1987, AJ, 93, 60
Sersic, J.L. 1968, Atlas de galaxias australes. Observatorio Astronomica, Cordoba
Simien, F., & de Vaucouleurs, G. 1986, ApJ, 302, 564
Struck-Marcell, C. 1991, ApJ, 368, 348
van den Bergh, S. 1989, PASP, 101, 1072
Wadadekar Y., Robbason R., & Kembhavi, A. 1999, AJ, 117, 1219

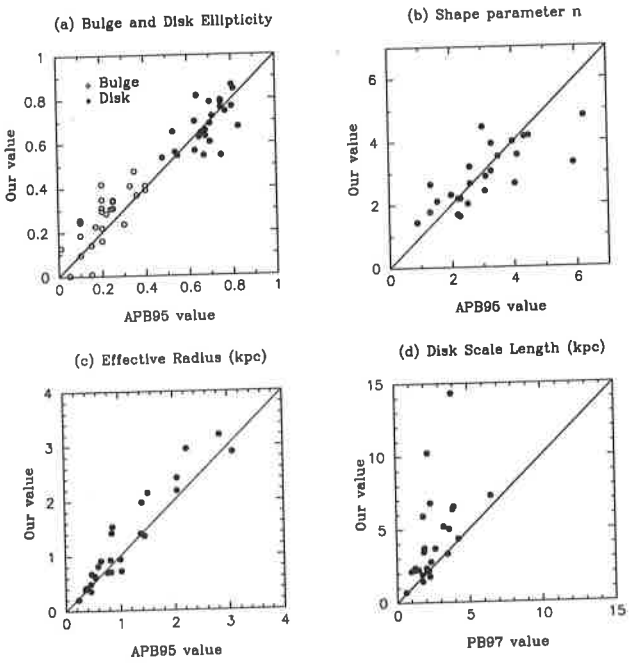

Fig. 1.— Comparison between extracted parameters from our decomposition program with those reported in the literature. (a) Bulge and disk ellipticity, (b) shape parameter n, (c) bulge effective radius and (d) disk scale length. Our results are compared with the results of APB95 in panels (a),(b) and (c) and with Peletier & Balcells (1997) in panel (d).

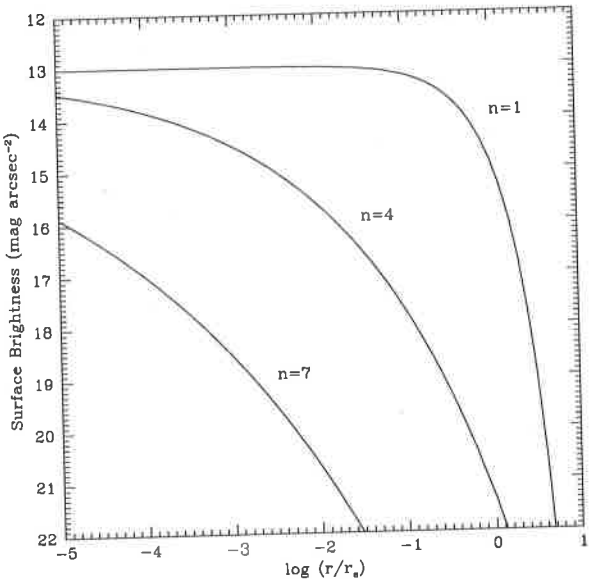

Fig. 2.— Bulge surface brightness profiles for $n = 1, 4, 7$. The profiles are in arbitrary units and have been normalized to central bulge intensity $I_b(0) = 1$.

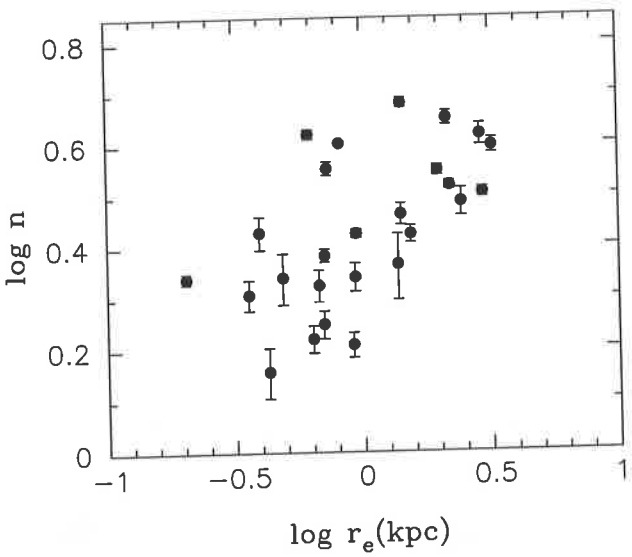

Fig. 3.— The bulge parameter n versus the bulge effective radius in kpc. The linear correlation coefficient is 0.61 at a significance level of 99.98 percent.

TABLE 1

EXTRACTED BULGE AND DISK PARAMETERS

Name	T^a	m^b	z^b	e_b	e_d	n	Δn	r_e (kpc)	r_d (kpc)	$\mu_b(0)$	$\mu_d(0)$	B/D
IC 1029	3	12.2	0.00795	0.41	0.79	2.19	0.14	0.93	10.25	10.96	16.94	0.09
NGC 5326	1	12.9	0.00841	0.31	0.54	1.66	0.10	0.63	2.19	11.83	15.51	0.30
NGC 5362	3	13.14	0.00726	0.41	0.57	2.31	0.34	1.36	3.72	12.92	17.04	0.06
NGC 5422	-2	12.81	0.00594	0.23	0.77	2.41	0.07	0.71	3.47	10.87	16.20	0.18
NGC 5475	0	13.50	0.00574	0.00	0.72	2.02	0.14	0.36	2.23	11.69	15.96	0.08
NGC 5587	0	13.51	0.00768	0.22	0.78	2.11	0.15	0.67	5.93	12.32	16.64	0.04
NGC 5675	0	13.70	0.01325	0.24	0.63	2.90	0.14	1.41	4.36	10.37	16.28	0.31
NGC 5689	0	12.8	0.00720	0.47	0.54	3.30	0.06	2.18	6.82	9.76	16.55	0.33
NGC 5707	2	13.30	0.00738	0.14	0.79	1.77	0.11	0.70	3.71	13.08	16.43	0.18
NGC 5719	2	13.26	0.00581	0.42	0.66	1.61	0.09	0.91	1.45	12.12	14.93	0.67
NGC 5838	-3	11.92	0.00455	0.19	0.70	2.66	0.05	0.94	2.78	10.66	17.00	0.79
NGC 5854	-1	12.71	0.00579	0.16	0.61	3.57	0.11	0.73	1.91	9.19	15.56	0.19
NGC 5866	-1	10.74	0.00224	0.25	0.81	4.00	0.05	0.82	2.14	9.83	14.83	0.44
NGC 5879	4	12.22	0.00258	0.37	0.69	2.19	0.05	0.20	0.71	11.56	14.81	0.03
NGC 5908	3	12.71	0.00579	0.24	0.85	4.47	0.14	2.14	5.17	9.21	14.73	0.08
NGC 5965	3	12.60	0.01138	0.39	0.68	3.94	0.13	3.20	6.54	9.56	16.14	0.19
NGC 5987	3	12.72	0.01004	0.34	0.63	3.53	0.08	1.97	5.00	9.13	16.06	0.37
NGC 6010	0	13.60	0.00630	0.28	0.74	2.19	0.25	0.49	2.19	10.60	15.41	0.19
NGC 6368	3	13.10	0.00922	0.01	0.55	4.15	0.20	2.88	3.33	9.83	15.95	0.15
NGC 6504	2	13.50	0.01597	0.31	0.86	3.20	0.07	2.95	7.29	10.19	15.98	0.25
NGC 6757	0	13.88	0.00710	0.10	0.56	2.68	0.20	0.39	2.38	10.31	16.27	0.13
NGC 7311	2	13.36	0.01512	0.13	0.65	2.65	0.10	1.53	6.35	10.25	16.18	0.28
NGC 7332	-2	12.02	0.00391	0.31	0.76	4.18	0.09	0.62	2.22	6.89	15.52	0.26
NGC 7457	-3	12.09	0.00271	0.35	0.54	4.80	0.10	1.42	2.38	8.65	16.87	0.26
NGC 7537	4	13.86	0.00892	0.35	0.65	1.43	0.16	0.43	1.79	14.23	15.41	0.03
NGC 7711	-2	13.07	0.01353	0.30	0.79	3.06	0.19	2.42	14.33	10.21	17.89	0.34

NOTE.—The columns are T: Morphological type index, m: apparent magnitude, z: redshift, e_b: bulge ellipticity, e_d: disk ellipticity, n: bulge shape parameter, Δn: error in n, r_e: bulge effective radius, r_d: disk scale length, $\mu_b(0)$: unconvolved bulge central surface brightness, $\mu_d(0)$: unconvolved disk central surface brightness, B/D: bulge-to-disk luminosity ratio.

[a]obtained from RC3.

[b]obtained from NED.

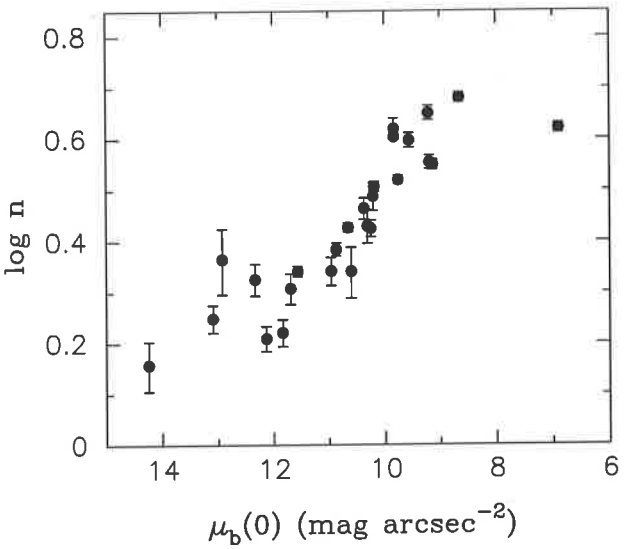

Fig. 4.— n as a function of the unconvolved bulge central surface brightness. The linear correlation coefficient is -0.88 at a significance level of over 99.99 percent.

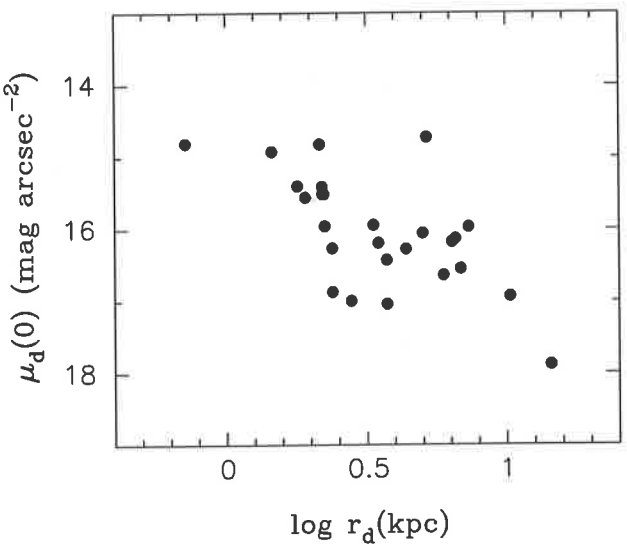

Fig. 6.— Unconvolved disk central surface brightness $\mu_d(0)$ as a function of disk scale length. An anti-correlation is seen with a linear correlation coefficient of 0.645 with a significance of 99.96 percent.

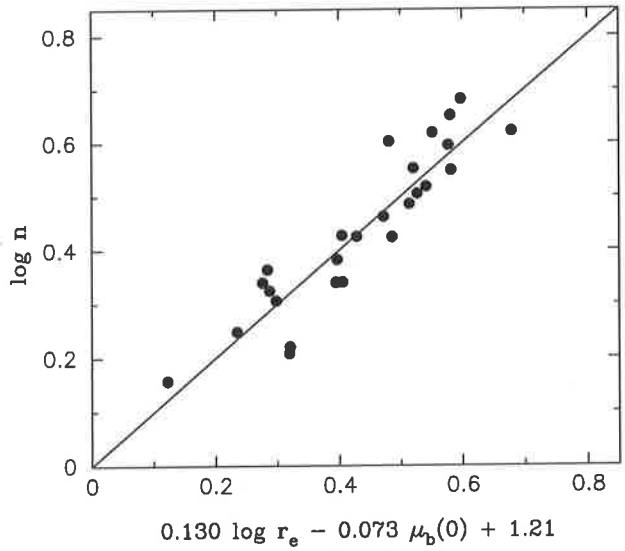

Fig. 5.— An empirical relation between n and the two other parameters of the bulge, r_e and $\mu_b(0)$. The solid line is the best fit line to the points. The scatter about the line is 0.058 dex in $\log n$.

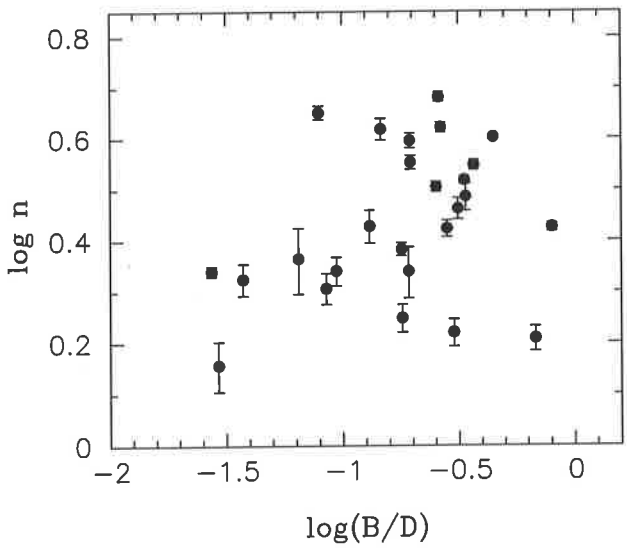

Fig. 7.— n versus bulge-to-disk ratio. The linear correlation coefficient is 0.30 with a significance of 86.5 percent.

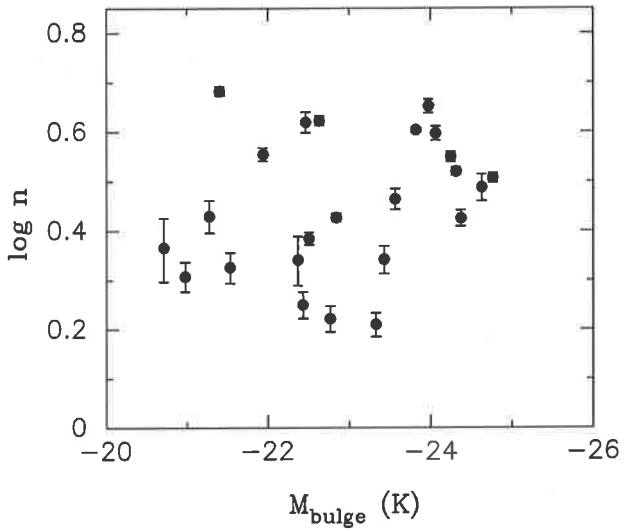

Fig. 8.— The best-fitting n versus bulge absolute magnitude in the K-band. The linear correlation coefficient is -0.40 at a significance level of 95.9 percent.

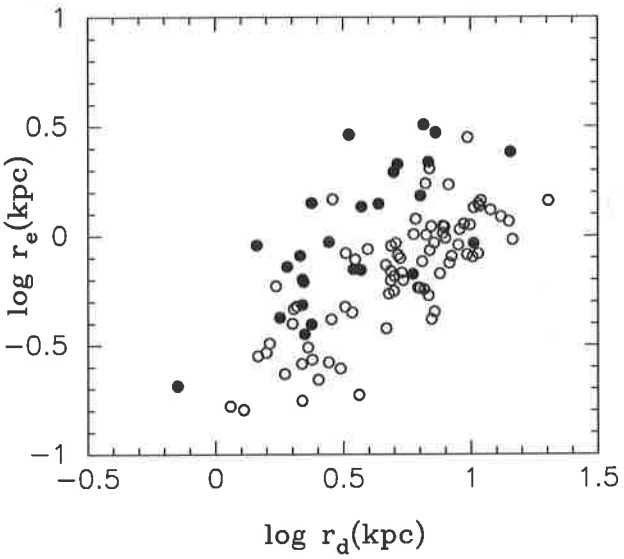

Fig. 10.— The dependence of bulge effective radius on disk scale length. The filled circles represent our sample, while the open circles are the K band data from de Jong (1996).

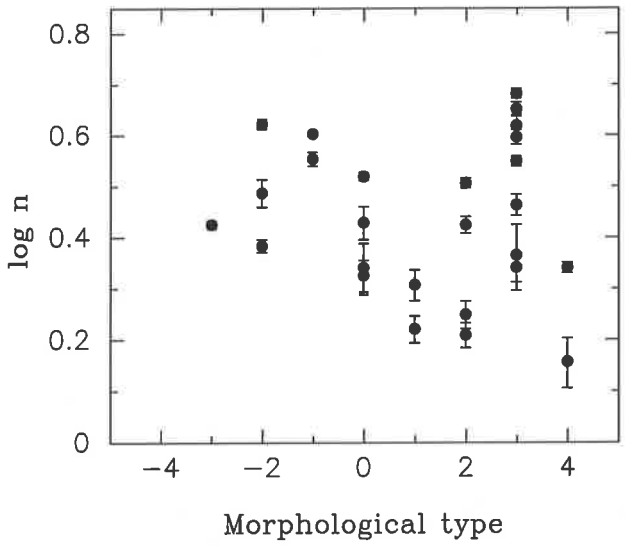

Fig. 9.— Shape parameter n versus morphological type.

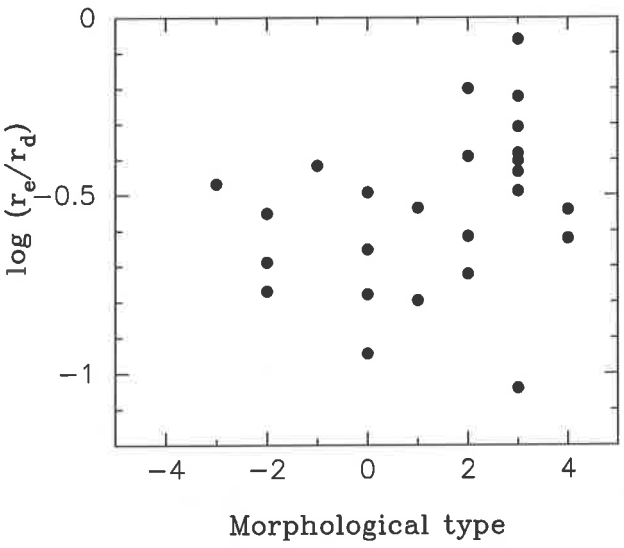

Fig. 11.— The variation of r_e/r_d ratio with morphological type.

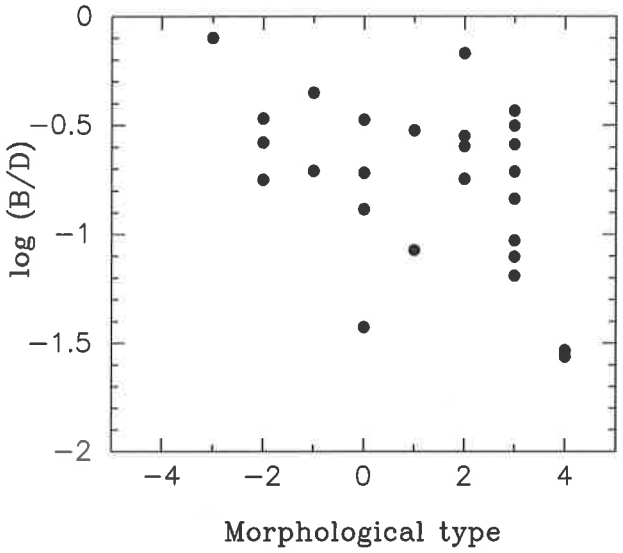

Fig. 12.— The variation of bulge-to-disk luminosity ratio with morphological type. An anti-correlation characteristic of the Hubble sequence is seen.

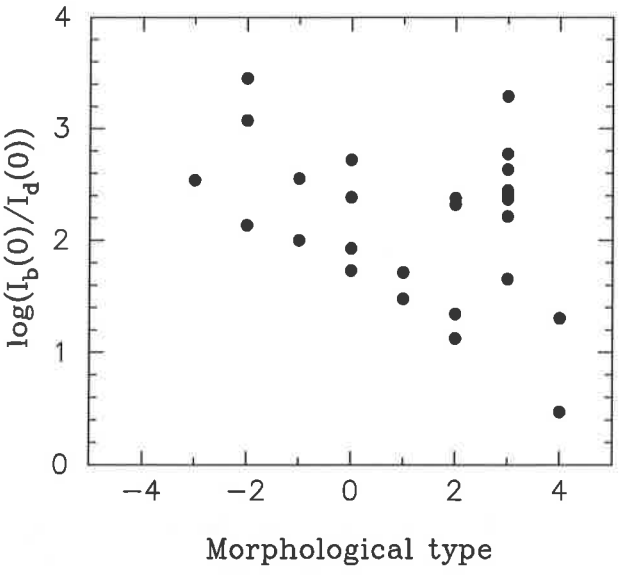

Fig. 13.— The dependence of bulge-to-disk central intensity ratio on morphological type.

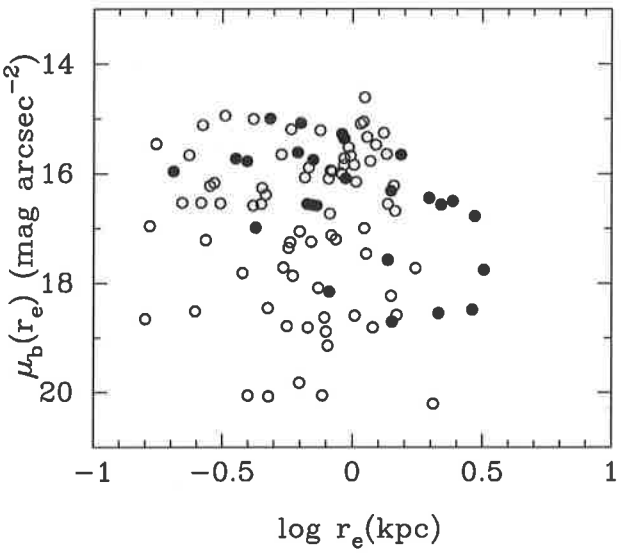

Fig. 14.— The dependence of the surface brightness at the effective radius $\mu_b(r_e)$ on r_e. The filled circles represent our sample while the open circles are the K band data from de Jong (1996).